(68)Ga-labeled superparamagnetic iron oxide nanoparticles (SPIONs) for multi-modality PET/MR/Cherenkov luminescence imaging of sentinel lymph nodes.

Madru, Renata; Tran, Thuy; Axelsson, Johan; Ingvar, Christian; Bibic, Adnan; Ståhlberg, Freddy; Knutsson, Linda; Strand, Sven-Erik

Published in:
American journal of nuclear medicine and molecular imaging

2014

Am J Nucl Med Mol Imaging 2014;4(1):60-69
www.ajnmmi.us /ISSN:2160-8407/ajnmmi1310004

Original Article

^{68}Ga-labeled superparamagnetic iron oxide nanoparticles (SPIONs) for multi-modality PET/MR/Cherenkov luminescence imaging of sentinel lymph nodes

Renata Madru[1], Thuy A Tran[1,2], Johan Axelsson[3], Christian Ingvar[4], Adnan Bibic[1], Freddy Ståhlberg[1,2,5], Linda Knutsson[1], Sven-Erik Strand[1,2]

[1]Department of Medical Radiation Physics, Lund University, Lund, Sweden; [2]Lund University Bioimaging Center, Lund University, Lund, Sweden; [3]Department of Physics, Lund University, Lund, Sweden; [4]Department of Surgery, Skane University Hospital, Lund, Sweden; [5]Department of Diagnostic Radiology, Lund University, Lund, Sweden

Received October 23, 2013; Accepted November 18, 2013; Epub December 15, 2013; Published January 1, 2014

Abstract: The aim of this study was to develop ^{68}Ga-SPIONs for use as a single contrast agent for dynamic, quantitative and high resolution PET/MR imaging of Sentinel Lymph Node (SLN). In addition ^{68}Ga enables Cherenkov light emission which can be used for optical guidance during resection of SLN. SPIONs were labeled with ^{68}Ga in ammonium acetate buffer, pH 5.5. The labeling yield and stability in human serum were determined using instant thin layer chromatography. An amount of 0.07-0.1 mL (~5-10 MBq, 0.13 mg Fe) of ^{68}Ga-SPIONs was subcutaneously injected in the hind paw of rats. The animals were imaged at 0-3 h and 25 h post injection with PET/CT, 9.4 T MR and CCDbased Cherenkov optical systems. A biodistribution study was performed by dissecting and measuring the radioactivity in lymph nodes, kidneys, spleen, liver and the injection site. The labeling yield was 97.3 ± 0.05% after 15 min and the ^{68}Ga-SPIONs were stable in human serum. PET, MR and Cherenkov luminescence imaging clearly visualized the SLN. Biodistribution confirmed a high uptake of the ^{68}Ga-SPIONs within the SLN. We conclude that generator produced ^{68}Ga can be labeled to SPIONs. Subcutaneously injected ^{68}Ga-SPIONs can enhance the identification of the SLNs by combining sensitive PET and high resolution MR imaging. Clinically, hybrid PET/MR cameras are already in use and ^{68}Ga-SPIONs have a great potential as a single-dose, tri-modality agent for diagnostic imaging and potential Cherenkov luminescent guided resection of SLN.

Keywords: ^{68}Ga, superparamagnetic iron oxide nanoparticle (SPION), sentinel lymph node (SLN), PET/MR imaging, Cherenkov imaging, lymphatics

Introduction

Solid tumors (carcinomas) mainly disseminate through the lymphatic system and the first metastases often arise in regional lymph nodes [1]. Therefore, the pathological status of the sentinel lymph node (SLN), defined as the first node receiving lymphatic drainage from the primary tumor site, provides important information of tumor progression [2]. SLN involvement is the most significant prognostic factor in breast cancer and melanoma patients [3, 4]. The clinical practice is to identify the SLN on lymphoscintigraphic images after periareolar injection of ^{99m}Tc labeled colloids, and then intraoperatively by using a handheld gamma probe. The SLNs are surgically removed and analyzed for the presence of tumor cells [5]. However, pre- and intraoperative identification of the SLN is challenging due to the low specificity and low uptake of the tracer (<1% of the injected activity) [6]. An injection of a blue dye is also administrated to guide the intraoperatively dissection of SLN [7]. Identification of the SLNs is limited by the small surgical field of view for nodal sampling and the lack of pre-operative anatomical images for surgical guidance which sometimes make the localization of the SLN difficult. This is particularly true in obese patients [8]. Furthermore, histopathological studies show that more than 64% of dissected SLNs are tumornegative [9]. Therefore, non-invasive,

sensitive and specific techniques for *in vivo* SLN diagnostics are warranted.

In the past decade several new tracers such as quantum dots, silica nanoparticles, liposomes and dendrimers in combination with or without fluorophores have been tested in animal models using different stand alone or hybrid imaging modalities [10]. However, the toxicity and *in vivo* stability of these tracers have not yet been fully evaluated. Another approach for pre-operative imaging was presented by Goldberg et al. and Sever et al. where micro-bubbles were used for the localization of SLN with ultrasound [11, 12]. For intraoperative guidance fluorescent dye such as indocyanine green (ICG) [13, 14] and reticuloendothelial-cell-specific receptor binding tracer, ^{99m}Tc-tilmanocept undergoing Phase III studies have been proposed [15]. Recent development includes optical imaging which detects Cherenkov luminescence, using radionuclides that emit beta-particles with electron energies higher than 219 keV [16, 17]. Thorek et al. and Park et al. presented intraoperative guidance for SLN resection using ^{18}F-FDG or ^{124}I-TCL-SPIONs in pre-clinical studies [18, 19]. In addition, instruments for endoscopic imaging of Cherenkov emission for surgical guidance have also been developed by Liu et al. [20].

One promising agent for SLN mapping is superparamagnetic iron oxide nanoparticles (SPIONs). SPIONs consist of a magnetic core coated with biocompatible material, which serve as an efficient contrast agent for MR imaging. SPIONs injected intravenously are retained in the reticuloendothelial system such as the liver, spleen and lymph nodes. Studies of patients with breast, head and neck, pelvic, and esophageal cancer have suggested that SPION enhanced-MRI can differentiate between healthy and metastatic SLNs *in vivo* [21, 22]. However, this technique suffers from low sensitivity. Additionally, SPIONs "negative" contrast properties make it difficult to identify the SLN in MR images. To overcome these problems, we previously suggested labeling the SPIONs with ^{99m}Tc which is useful for high sensitivity SPECT and high resolution MR in pre-surgical identification of SLNs [23]. The excellent properties of the ^{99m}Tc-SPIONs, shown in that paper, encourage further development in order to combine SPIONs and PET tracers for PET-MR imaging. The inclusion of PET would benefit the sensitivity and generate quantitative images and can also make use of current hybrid PET/MR system development. ^{68}Ga can be obtained from ^{68}Ge/^{68}Ga generators, which are highly available and easy to implement in the clinical infrastructure.

Here we present a triple-modality imaging agent, ^{68}Ga-SPIONs, administrable in a single injection for PET-MR SLN mapping. Additionally, ^{68}Ga-SPIONs enable Cherenkov light emission due to the high energy of the emitted positrons useful for optical guidance at surgery. The aim of this study was to develop a labeling method for ^{68}Ga-SPIONs and demonstrate the feasibility for all three modalities to pre- and intraoperatively identify and localize SLNs.

Material and method

Radiolabeling

The SPION nanoparticles (Genovis AB, Sweden) have been described previously in a paper by Madru et al. [23]. Briefly, they are composed of spherical monodispersed iron oxide cores composed of Fe_3O_4 (~13 nm in diameter measured by transmission electron microscopy) and coated with biocompatible and functionalized polyethylene glycol (PEG). The coated nanoparticles have a hydrodynamic diameter of 30 nm (SD 3 nm) and provides a strong T2 and T2* relaxation based contrast in MR images.

^{68}Ga ($T_{1/2}$=67.7 min, β^+=89% and EC=11%) was available from a ^{68}Ga/^{68}Ge-generator system (IDB, Holland). ^{68}Ga was eluted with 6 mL of 0.6 M hydrochloric acid in 0.3-0.4 mL fractions. A fraction containing 40-80 MBq of $^{68}GaCl_3$ in a volume of ~0.3 mL was used for labeling.

To determine the optimal pH for the labeling, three buffering agents were used in order to obtain the required pH values of 3.5, 5.5, 7 and 9. Sodium acetate (0.4 M), HEPES (0.6 M), and ammonium acetate (1 M) was added to ~0.4 mL $^{68}GaCl_3$ and the pH was (if required) furthermore adjusted with HCl (0.6 M) and NaOH (10 M). SPIONs in physiological saline (40 μL, 1.4 mg Fe) were mixed with 40 μL of the buffering agent (pH 3.5, 5.5, 7 or 9) and added to the vial with the ^{68}Ga-buffer (corresponding pH as mentioned above). The pH was monitored with pH test strips (3 steps, Sigma, USA and Merck, Germany). The reaction mixture was incubated in a heating box under gentle shaking conditions at 50°C for 25 min.

Quality control: Samples were taken at 5, 10, 15 and 25 min post labeling and analyzed for radioactivity incorporation by instant thin layer chromatography (ITLC, TEC-control chromatography strips, Biodex, USA) using 0.2 M citric acid as running buffer. The ITLC strips were imaged by a phosphor imager (Welesley, MA, Perkin Elmer, USA). A phosphor storage plate (Multisensitive, medium, Perkin Elmer, USA) was placed on the top of the strips and exposed for 5 minutes. The plate was scanned and analyzed using the OptiQuant image analysis software (Perkin Elmer, USA).

The labeling efficiency was also evaluated by separating the ^{68}Ga-SPIONs from the reaction mixture with a column containing ferromagnetic spheres (Miltenyi Biotech, Germany). Attaching a magnet to the column and filtering the reaction mixture, the ^{68}Ga-SPIONs were trapped within the column while the free ^{68}Ga and buffer solution flow through. The magnet was removed and the ^{68}Ga-SPIONs were eluted with sterile water, saline or ammonium acetate buffering solution. The radioactivity of the ^{68}Ga-SPIONs was compared with the activity of the free ^{68}Ga by using a dose calibrator (Atomlab 500, Biodex, USA).

The labeling stability studies were performed by incubating the ^{68}Ga-labeled SPIONs in human serum (pH 7) at 37°C for 60, 120, 180 and 240 min and analyzed with ITLC as described previously. The experiments were performed in triplicate.

Animal studies

White Wistar rats (n=9, Charles River, Germany) with weight 250-300 g were used in compliance with local and national regulations approved by the Local Ethics Committee for Animal Research, Lund, Sweden. The animals were anesthetized with 2-3% isoflurane during injection and imaging and the ^{68}Ga-SPIONs in ammonium acetate buffer (pH 5.5) or physiological saline (3-10 MBq equivalents to 0.05-0.07 mL, ~0.13 mg Fe) was subcutaneously injected in the right hind paw. The contralateral side served as control.

PET/CT imaging: To evaluate the *in vivo* biodistribution of ^{68}Ga-SPIONs the injected animals were placed on an animal bed and imaged with a dual-modality, positron emission tomography and computed tomography system (PET/CT, NanoPET/CT, Bioscan, USA). The injection site was covered with a lead plate during imaging sessions in order to eliminate possible interfering with the adjacent SLN. The PET images were collected in 10-15 min intervals or as a dynamic PET acquisition performed up to 3 h. Reconstruction of the images was made by using ordered subset expectation maximum (OSEM) iterative method with the following parameters: energy window 400-600 keV, single slice rebinning to 2D LOR, ring difference 16 and coincidence 1-3. Morphological information was provided by CT images acquired with 55 kV, 360 projections, medium or maximum zoom and reconstructed with RamLack filter. The PET and CT images were sent to a workstation for coregistration and analysis (InVivoscope, Bioscan USA). One animal was returned to its cage and was sacrificed the next day (25 h post injection). Five animals were sacrificed by an overdose of isoflurane at the end of the PET/CT scan.

MR imaging: Two of the sacrificed animals were imaged in a horizontal bore MR scanner 3 h and 25 h p.i. (9.4 T Agilent Palo Alto, CA, USA) using a transmit/receive, 72 mm inner diameter volume coil (Rapid Biomedical GmbH, Rimpar, Germany). The images were acquired using PD-weighted 3D gradient-echo (3D-GRE) pulse sequence with the following parameters: TR=9.50 ms, TE=2.53 ms, number of average (NA)=4, flip angle 6 degrees, field of view=113 mm × 58.5 mm × 66.3 mm, Matrix 512 × 512 × 256.

Optical imaging: Three animals were used for optical imaging after the PET/CT scan. Cherenkov fluorescence imaging was performed by using a slow-scan deep-cooled CCD camera (Andor iKon 934 M, Andor, Ireland). The camera was equipped with an objective lens of focal length 25 mm and f-number 0.95 (Xenon, Schneider Kreuznach, Germany). The camera was placed in a light tight enclosure to suppress ambient room light. Cherenkov emission images of the animals employed 8 × 8 binning and an exposure time of 10 min or 2 min.

In order to ensure the linearity of Cherenkov radiance with ^{68}Ga activity, a well plate was imaged containing 1.2 mL water, 0.2 mL scattering liquid (20% - Intralipid©, Fresenius-Kabi, Sweden) to mimic the scattering properties of

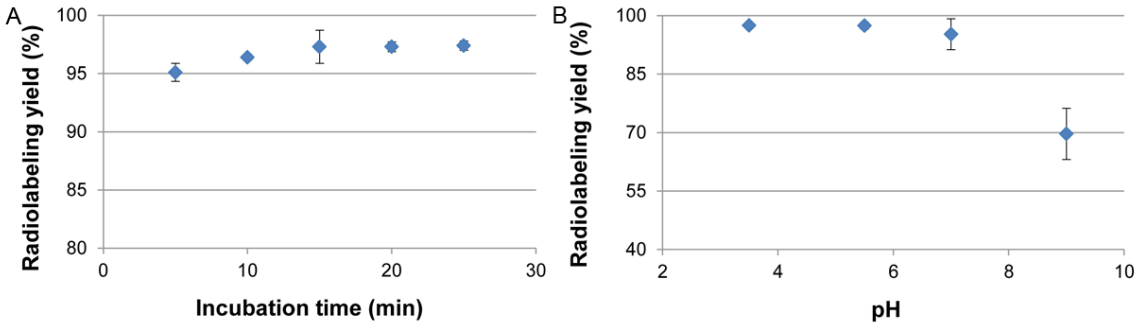

Figure 1. Radiolabeling of the ^{68}Ga-SPIONs. A: The Radiolabeling yield in ammonium acetate buffer (pH 5.5) exceeded 95% (n=3) after 10 minutes of incubation time. B: The radiolabeling yield is shown to be optimal when the labeling of ^{68}Ga-SPIONs is performed at pH 3-7 (n=3).

tissue, and ^{68}Ga with activity concentrations varying from 0.098 MBq to 1.79 MBq. The well plate images employed 4 × 4 binning and exposure times of 10 min. All Cherenkov emission images were subject to median filtering to remove the hotspots from the registered gamma photons.

Biodistribution

Four animals were dissected immediately after the PET/CT imaging where lymph nodes, kidneys, spleen, liver and the hind paw containing the injection site were removed, weighed and measured for radioactivity in a NaI(Tl) well-type detector (1282 CompuGamma CS; LKB Wallac). All measurements were corrected for background and radioactive decay. The accumulation of the ^{68}Ga-SPIONs in the dissected organs was expressed as the percentage injected activity per gram wet tissue (% IA/g).

Results

Radiolabeling

The ammonium acetate buffer (1 M, pH 5.5) was found optimal for ^{68}Ga labeling of SPIONs. The radiolabeling efficiency, as determined by ITLC was >95% within 10 min and reaching a plateau of 97.3 ± 0.05% after 15 min incubation at 50°C (**Figure 1A**, **1B**). The radiolabeled SPIONs remained at the origin on the ITLC sheets, whereas free ^{68}Ga moved with the solvent front at an R_f value of 0.9. Similar results, 97% labeling efficiency after 15 minutes incubation, were found with the magnetic separation method. ^{68}Ga-SPIONs were stable in human serum (pH 7, >93%) at 37°C for 4 h. The labeling efficiency was found to be 95 ± 3% in HEPES buffer at pH 3.5 and 87 ± 1.7% in sodium acetate buffer at pH 4 after 25 minutes of incubation at 50°C.

Animal studies

PET/CT imaging: The accumulation of the ^{68}Ga-SPIONs within the SLN (popliteal node) was detectable with PET within 30 min. The anatomical information provided from the coregistration with CT images confirmed that the ^{68}Ga-SPIONs were localized within the lymph node (**Figure 2A**, **2B**). A small amount of radioactivity could be visualized in the second (iliac) lymph node (3 h p.i.), in good agreement with the biodistribution data.

MRI imaging: To demonstrate the potential of ^{68}Ga-SPIONs for future simultaneous PET/MR imaging, the animal bed with the rat was removed from the PET system and moved into the MR camera and imaged with the GRE sequence (image parameters described above). The MR image visualizing the SLNs is shown in **Figure 3A**. The SLN on the right side could be recognized due its hypointensity, compared with the reference node. The MR image showed good delineation of the SLN. **Figure 3B** shows the presence of the SPIONs 25 h p.i., with a somewhat more homogenous uptake within the SLN compared with **Figure 3A**. Even in this image a good delineation of the node is demonstrated and no obvious "blooming artifacts" are present that could be caused by the iron oxide core.

Cherenkov imaging: Cherenkov emission images of ^{68}Ga-SPIONs (3 h p.i., ~15 MBq injected activity) are shown in **Figure 4A**. The rat skin

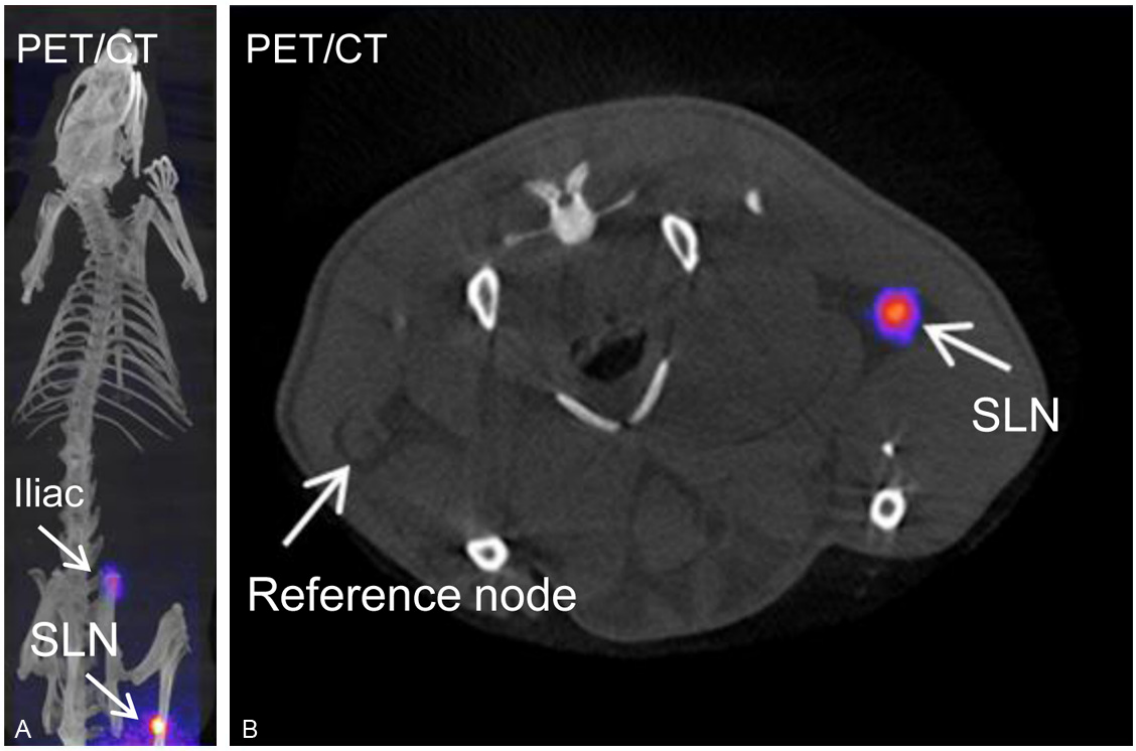

Figure 2. PET/CT image of one representative animal. A: Fused whole-body image of the rat 3 h after subcutaneous injection with ^{68}Ga-SPIONs. The arrows show accumulation of ^{68}Ga-SPIONs in the SLN (popliteal) and iliac node. B: The axial image visualizing the SLN in comparison with the contralateral reference node.

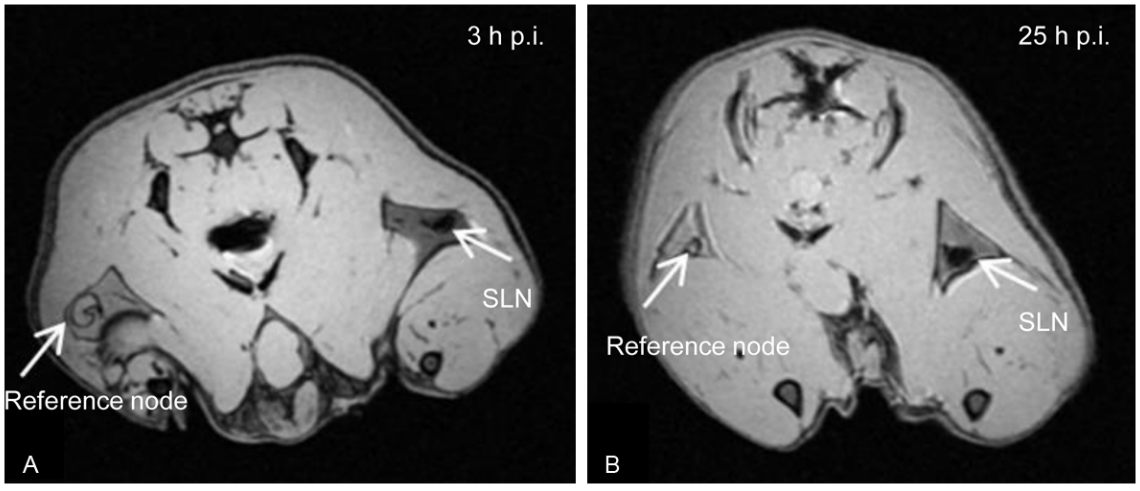

Figure 3. MR imaging of rats visualizing the SLN. A: Axial MR image of the same animal as shown in **Figure 2**. The uptake of the ^{68}Ga-SPIONs in SLN after 3 h is evidently seen in the image. B: The SLN are clearly visualized indicating hypointensity due to accumulation of the ^{68}Ga-SPIONs, 25 h after injection.

was shaved but intact rendering a low radiance due to the large penetration depth. The exposure time was 10 minutes. In **Figure 4B** the skin was removed leading to a stronger Cherenkov radiance in the image acquired using a short exposure time of 2 minutes. In **Figure 4C** a representative image of the Cherenkov emission from a well plate filled with the tissue mimicking liquid solution is shown. The extracted radiance from each well and plotted for different levels of activity show an excellent linearity as demonstrated in **Figure 4D**.

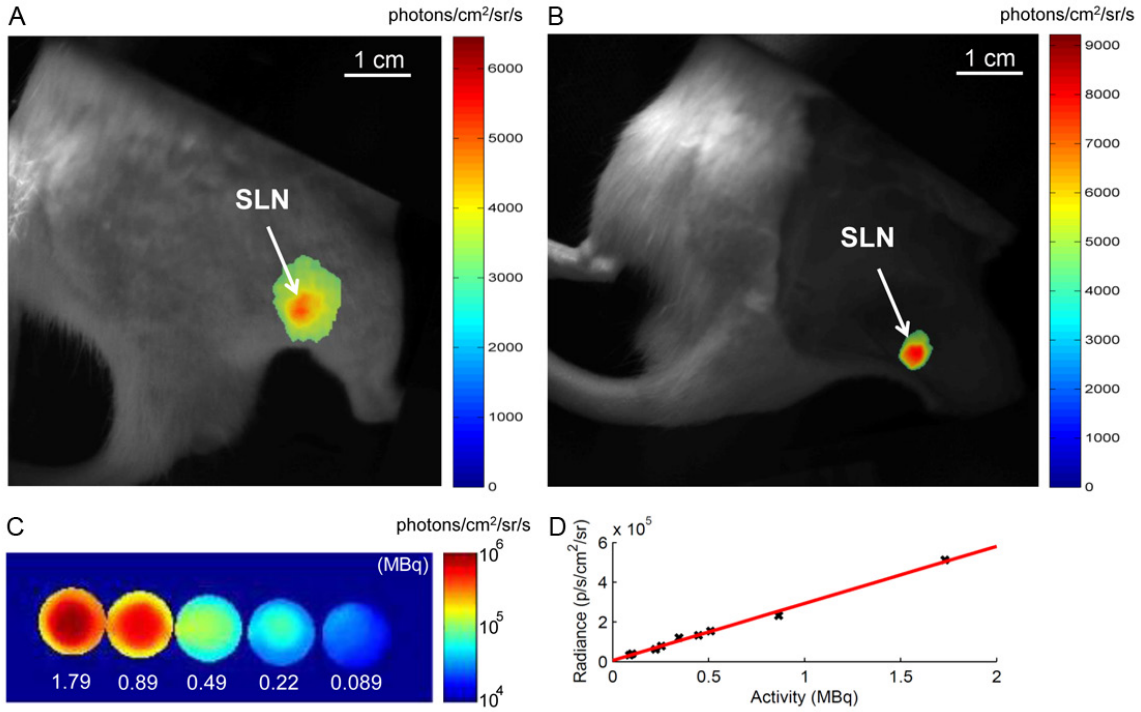

Figure 4. Optical images of ^{68}Ga-SPIONs visualizing the SLN 2.5-3 h p.i. A: Cherenkov emission image, 10 min exposure, where the skin was shaved but intact. B: Cherenkov emission image, 2 min exposure, after the skin was removed. C: Representative Cherenkov emission image, 2 min exposure, of a well plate filled with ^{68}Ga mixture with 20% Intralipid. The activity levels in the range of 0.08-1.8 MBq for each well are as indicated in the figure. D: The Cherenkov radiance plotted for the different levels of activity as extracted from each well. The linear relation is confirmed with an R2-value of 0.99. White bar in **Figure 4A**, **4B** indicates the length scale 10 mm.

Biodistribution: The clearance of the ^{68}Ga-SPIONs from the injection site was between 20 and 30%, 3 h after injection. The mean uptake in the lymph nodes, spleen, liver and kidneys is shown in **Figure 5**. The radioactivity uptake of the ^{68}Ga-SPIONs was highest in the SLN with 123% IA/g when in the second (iliac) node retained a mean of 47% IA/g. Organs of the reticuloendothelial system as liver and spleen had a low uptake of 0.3% IA/g respectively 0.1% IA/g, 3 h p.i. The kidneys retained a mean of 0.05% IA/g.

Discussion

SLN mapping using ^{99m}Tc-labeled colloids and blue dye has been widely accepted as a standard method, mostly for its reasonable detection rate, availability and low cost. However, these tracers are not specific and give no information regarding the pathological status of the lymph nodes. Lymphoscintigraphic images have low resolution and lack anatomical information for accurate localization of the SLN. Identification of the SLN is particularly difficult in malignant melanoma patients where the primary tumor may drain to several distant nodes. Recently, agents including micro-bubbles using ultrasound, ICG-fluorescent dye or ^{99m}Tc-tilamnocept have been suggested to identify the SLN. Pre-operative sonographic examination of axillary nodes in combination with biopsy suggested that the technique may identify metastatic involvement in SLN, however has low sensitivity (53.7%) and accuracy (67.9%) which not justifies its clinical use [24]. The use of micro-bubbles, however may enhance the detection rate of the SLN (up to 89%) as demonstrated by Sever in a study of 80 breast cancer patients. The ICG-fluorescent methods using standard CCD imaging instrument show a high detectability of over 90% of the SLN but cannot differentiate between normal- and nodes with tumor involvement [25]. ^{99m}Tc-tilamnocept has the main advantage of its small molecular size which leads to a rapid clearance from the injection site and selective accumulation in SLNs within 20 minutes.

Other agents with potential to identify metastatic involvement in SLNs are those containing

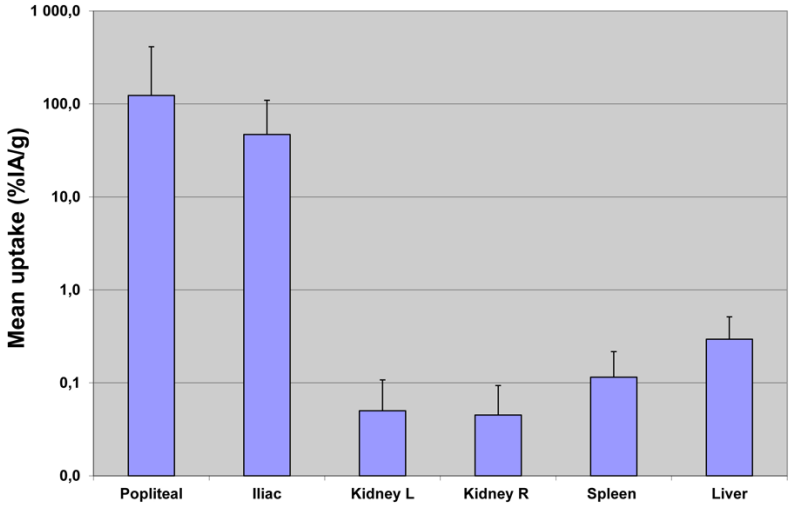

Figure 5. Biodistribution data of ^{68}Ga-SPIONs in 4 white Wistar rats 3 h after subcutaneous injection in the right hind paw. Uptake is shown as mean ± SD % IA/g.

SPIONs used for MR imaging. SPIONs cause a shortening of the transversal relaxation of the spins and introducing a local field inhomogeneity within the SLN which leads to the decrease of the signal, generating "dark nodes" in MR images. Metastatic nodes however, with an inhomogeneous accumulation of SPIONs within the SLN will not be homogenously darkened. Other advantage compared to the ^{99m}Tc-labeled colloids is that SPIONs can be produced in a systematic way with the desired diameter in a narrow size range, crucial for SLN imaging [26].

With this in mind we choose to work with SPIONs and designed a single agent, ^{68}Ga-SPIONs for multiple imaging purposes. Firstly, it enables localization of SLN with sensitive PET and high resolution MR imaging. Secondly, ^{68}Ga-SPIONs enables Cherenkov luminescence optical guided SLN surgery.

Similarly to generator produced ^{99m}Tc, the positron emitter ^{68}Ga will be available from an in-house ^{68}Ge/^{68}Ga generator, making it attractive for sites without cyclotrons. Additionally, ^{68}Ga has favorable physical properties (half-life of 68 minutes, 89% β^+ emission) and easy chelate-mediated or direct labeling chemistry [27, 28]. Due to its superior imaging properties, ^{68}Ga-DOTA-octreotides have already replaced the ^{99m}Tc/^{111}In-DTPA-octreotides used for imaging of neuroendocrine tumors [29]. ^{68}Ga-labeled peptides have also been successfully used for visualization of different inflammatory diseases [30] which demonstrates that ^{68}Ga is a promising candidate in the modern era of "personalized medicine".

In this study, ^{68}Ga is attached to SPIONs with direct labeling method. Ammonium acetate was found to be the most suitable buffer solution for labeling, with a labeling efficiency over 97% within 15 minutes. The labeling yield was found highest at pH 3-5.5. ^{68}Ga-SPIONs were found to have a good dispersion in buffer agents and to be stable in human serum (up to 4 h) which encouraged to in vivo applications using white Wistar rats. ^{68}Ga-SPIONs injected subcutaneously in the right hind paw of the rats was transported within the lymphatic vessels and retained in SLN as demonstrated in PET, MR and Cherenkov luminescence images.

In PET images **Figure 2A**, **2B**, the activity within the SLN was well correlated with the ex vivo biodistribution study and show that there was about three times more activity in the first node compared with the second lymph node. MR images taken 25 h after injection demonstrates that the ^{68}Ga-SPIONs are still present in the SLN in high concentration which may enable second day protocols in clinic. No image artifacts have been detected around the SLN as demonstrated in **Figure 3A** and **3B**. However, due to the "negative" contrast in MR images, localization of the SLNs in patients could be difficult, and the results suggest that there is a need to label the SPIONs with ^{68}Ga in order to improve the overall (pre- and intraoperative) SLN detectability.

Optical imaging using ^{68}Ga-SPION as a source for Cherenkov emission can potentially find a role as a tool for intra-operative surgical guidance. However, the optical photons are affected by the optical attenuation as well as the depth of emission. In order to battle the ever present optical attenuation there is a need for radionuclides that can generate strong Cherenkov emission. In this work the radionuclide

^{68}Ga is responsible for emission of Cherenkov light. In comparison to previously reported studies, the beta particles emitted from ^{68}Ga have much higher energy (Max. 1.89 MeV) compared with ^{18}F (0.634 MeV) and ^{124}I (0.819 MeV). This higher energy leads to a stronger Cherenkov emission [30]; hence the use of ^{68}Ga can enable identification of SLN localized deeper in the tissue.

The clearance of the ^{68}Ga-SPION from the injection site was found to be comparable to the clearance of ^{99m}Tc-SPIONs used in our previous study for SPECT/MR imaging of the SLNs (~20% 3 h post injection) [23], demonstrating that the clearance mainly depends on the size and the coating of the SPIONs and is less affected by the attached radionuclide. The mean uptake of ^{68}Ga-SPION in SLN was over 2% with the lowest value of 0.8% and highest 6.3%, three hours post injection. This can be compared to the mean value of 1.72%, the lowest value 0.4% and the highest 4.0% for ^{99m}Tc-SPIONs, 4 h after injection. Individual variations observed in uptake, probably occurred as an influence of the anesthesia. The biodistribution data shows that a small amount of ^{68}Ga-SPION was transported through the lymphatic system and other nodes and finally accumulated in liver and spleen. PET compared to SPECT imaging offers advantages such as better spatial resolution and quantitative images. Due to the higher sensitivity, PET allows much shorter scanning times than SPECT.

Conclusion

In this study, a fast one step labeling method of SPIONs with generator produced ^{68}Ga was demonstrated. Hybrid PET-MR systems are already available for both preclinical and clinical use which encourage the development of this kind of probes. Our results reveal that the first lymph node draining the injection site was clearly visible on PET, MR and Cherenkov images demonstrating the potential of this agent as a novel multimodality probe.

Acknowledgements

This study was performed with generous support from the Swedish Cancer Foundation, the Swedish Science Council, Mrs. Berta Kamprad's Foundation, Gunnar Nilsson's Foundation, and the ALF Foundation of the Medical Faculty of Lund University. The SPIONs were provided as a generous from Genovis AB, Sweden. The authors also want to thank Tomas Olsson for Ga-68 eluate for this study. Lund University Bioimaging Center (LBIC), Lund University is gratefully acknowledged for providing experimental resources.

Disclosure of conflict of interest

The SPIONs were a generous gift by Genovis AB.

Address correspondence to: Renata Madru, Department of Medical Radiation Physics, Skane University Hospital Lund, Lund University, SE-221 85 Lund, Sweden. Tel: +46 734 337608; Fax: +46 461 78540; E-mail: Renata.Madru@med.lu.se

References

[1] Alitalo K, Tammela T, Petrova TV. Lymphangiogenesis in development and human disease. Nature 2005; 438: 946-953.

[2] Civantos FJ, Zitsch RP, Schuller DE, Agrawal A, Smith RB, Nason R, Petruzelli G, Gourin CG, Wong RJ, Ferris RL, El Naggar A, Ridge JA, Paniello RC, Owzar K, McCall L, Chepeha DB, Yarbrough WG, Myers JN. Sentinel lymph node biopsy accurately stages the regional lymph nodes for T1-T2 oral squamous cell carcinomas: results of a prospective multi-institutional trial. J Clin Oncol 2010; 28: 1395-1400.

[3] Wong SL, Balch CM, Hurley P, Agarwala SS, Akhurst TJ, Cochran A, Cormier JN, Gorman M, Kim TY, McMasters KM, Noyes RD, Schuchter LM, Valsecchi ME, Weaver DL, Lyman GH. Sentinel lymph node biopsy for melanoma: American Society of Clinical Oncology and Society of Surgical Oncology joint clinical practice guideline. J Clin Oncol 2012; 30: 2912-2918.

[4] McMasters KM, Tuttle TM, Carlson C, Brown CM, Noyes RD, Glaser RL, Vennekotter DJ, Turk PS, Tate PS, Sardi A, Cerrito PB, Edwards MJ. Sentinel lymph node biopsy for breast cancer a suitable alternative to routine axillary dissection in multi-institutional practice when optimal technique is used. J Clin Oncol 2000; 18: 2560-2566.

[5] Balch CM, Gershenwald JE, Soong SJ, Thompson JF, Atkins MB, Byrd DR, Buzaid AC, Cochran AJ, Coit DG, Ding S, Eggermont AM, Flaherty KT, Gimotty PA, Kirkwood JM, McMasters KM, Mihm MC Jr, Morton DL, Ross MI, Sober AJ, Sondak VK. Final version of 2009 AJCC melanoma staging and classification. J Clin Oncol 2009; 27: 6199-6206.

[6] Silverio AM, McRae MC, Ariyan S, Narayan D. Management of the difficult sentinel lymph

node in patients with primary cutaneous melanoma. Ann Plast Surg 2010; 65: 418-424.
[7] Buscombe J, Paganelli G, Burak ZE, Waddington W, Maublant J, Prats E, Palmedo H, Schillaci O, Maffioli L, Lassmann M, Chiesa C, Bombardieri E, Chiti A. Sentinel node in breast cancer procedural guidelines. Eur J Nucl Med Mol Imaging 2007; 34: 2154-2159.
[8] Armer J, Fu MR, Wainstock JM, Zagar E, Jacobs LK. Lymphedema following breast cancer treatment, including sentinel lymph node biopsy. Lymphology 2004; 37: 73-91.
[9] Intra M, Rotmensz N, Mattar D, Gentilini OD, Vento A, Veronesi P, Colleoni M, De Cicco C, Cassano E, Luini A, Veronesi U. Unnecessary axillary node dissections in the sentinel lymph node era. Eur J Cancer 2007; 43: 2664-2668.
[10] Ratnesh J, Prajakta D, Vandana P. Diagnostic nanocarriers for sentinel lymph node imaging. J Control Release 2009; 138: 90-102.
[11] Goldberg BB, Merton DA, Liu JB, Thakur M, Murphy GF, Needleman L, Tornes A, Forsberg F. Sentinel lymph nodes in a swine model with melanoma: contrast-enhanced lymphatic US. Radiology 2004; 230: 727-734.
[12] Sever AR, Mills P, Jones SE, Mali W, Jones PA. Sentinel node identification using microbubbles and contrast-enhanced ultrasonography. Clin Radiol 2012; 67: 687-694.
[13] Van der Vorst JR, Scgaafsma BE, Verbeek FB, Hutteman M, Mieog JS, Lowik CW, Liefers GJ, Frangioni JV, van de Velde CJ and Vahrmeijer AL. Randomized comparison of near infrared fluorescence imaging using indocyanine green and 99(m) technetium with or without patent blue for sentinel lymph node procedure in breast cancer patients. Ann Surg Oncol 2012; 19: 4104-4111.
[14] Nguyen QT, Tsien R. Fluorescence-guided surgery with live molecular navigation - a new cutting edge. Nat Rev Cancer 2013; 13: 653-662.
[15] Emerson DK, Limmer KK, Hall DJ, Han SH, Eckelman WC, Kane CJ, Wallace AM, Vera DR. A receptor-targeted fluorescent radiopharmaceutical for multireporter sentinel lymph node imaging. Radiology 2012; 265: 186-193
[16] Robertson R, Germanos MS, Li C, Mitchell GS, Cherry SR, Silva MD. Optical imaging of Cerenkov light generation from positron-emitting radiotracers. Phys Med Biol 2009; 54: 355-365.
[17] Holland JP, Normand G, Ruggiero A, Lewis JS, Grimm J. Intraoperative imaging of positron emission tomographic radiotracers using Cerenkov luminescence emissions. Mol Imaging 2011; 10: 177-186.
[18] Thorek DLI, Robertson R, Bacchus WA, Hahn J, Rothberg J, Beattie BJ, Grimm J. Cerenkov imaging - a new modality for molecular imaging. Am J Nucl Med Mol Imaging 2012; 2: 163-173.
[19] Park JC, Yu MK, An GI, Park SI, Oh J, Kim HJ, Kim JH, Wang EK, Hong IH, Ha YS, Choi TH, Jeong KS, Chang Y, Welch MJ, Jon S, Yoo J. Facile preparation of a hybrid nanoprobe for triple-modality optical/PET/MR imaging. Small 2010; 6: 2863-2868.
[20] Liu H, Carpenter CM, Jiang H, Pratx G, Sun C, Buchin MP, Gambhir SS, Xing L and Cheng Z. Intraoperative imaging of tumors using Cerenkov luminescence endoscopy: A feasibility experimental study. J Nucl Med 2012; 53: 1579-84.
[21] Harisinghani MG, Saini S, Slater GJ, Schnall MD, Rifkin MD. MR imaging of pelvic lymph nodes in primary pelvic carcinoma with ultrasmall superparamagnetic iron oxide (Combidex): preliminary observations. J Magn Reson Imaging 1997; 7: 161-163.
[22] Nishimura H, Tanigawa N, Hiramatsu M, Tatsumi Y, Matsuki M, Narabayashi I. Preoperative esophageal cancer staging: magnetic resonance imaging of lymph node with ferumoxtran-10, an ultrasmall superparamagnetic iron oxide. J Am Coll Surg 2006; 202: 604-611.
[23] Madru R, Kjellman P, Olsson F, Wingårdh K, Ingvar C, Ståhlberg F, Olsrud J, Lätt J, Fredriksson S, Knutsson L, Strand SE. 99mTc-labeled superparamagnetic iron oxide nanoparticles for multimodality SPECT/MRI of sentinel lymph nodes. J Nucl Med 2012; 53: 459-463.
[24] Lee B, Lim AK, Krell J, Satchitananda K, Coombes RC, Lewis JS and Stebbing J. The efficiency of axillary ultrasound in the detection of nodal metastasis in breast cancer. AJR AM J Roentenol 2013; 200: 314-320.
[25] Wishart GC, Loh SW, Jones L and Benson JR. A feasibility study (ICG-10) of indocyanine green (ICG) fluorescence mapping for sentinel node detection in early breast cancer. Eur J Surg Oncol 2012; 38: 651-656.
[26] Anzai Y, Blackwell KE, Hirschowitz SL, Rogers JV, Sato J, Yuh WT, Runge VM, Morris MR, McLachlan SJ and Lufkin RB. Initial clinical experience with dextran-coated superparamagnetic iron oxide for detection of lymph node metastases in patients with head and neck cancer. Radiology 1994; 192: 709-715
[27] Velikyan I, Beyer GJ, Långström B. Microwave-supported preparation of 68Ga bioconjugates with high specific radioactivity. Bioconjug Chem 2004; 15: 554-560.
[28] Blom E, Velikyan I, Estrada S, Hall H, Muhammad T, Ding C, Nair M, Långström B. 68Ga-Labeling of RGD peptides and biodistribution. Int J Clin Exp Med 2012; 5: 165-172.
[29] Naji M, AL-Nahhas A. 68Ga-labelled peptides in the management of neuroectodermal tumours. Eur J Nucl Med Mol Imaging 2012; 39: S61-67.

[30] Li X, Samnick S, Lapa C, Israel I, Buck AK, Kreissl MC, Bauer W. 68Ga-DOTATATE PET/CT for the detection of inflammation of large arteries: correlation with 18F-FDG, calcium burden and risk factors. EJNMMI Res 2012; 2: 52.

[31] Glass EC, Essner R, Morton DL. Kinetic of three lymphoscintigraphic agents in patients with cutaneous melanoma. J Nucl Med 1998; 39: 1185-1190.